



Istituto Nazionale di Astrofisica
National Institute For Astrophysics
Osservatorio Astronomico di Torino




RAPPORTO TECNICO - TECHNICAL REPORT

Report No: 87/2007

L. Corcione, D. Bonino, M. Gai,
S. Ligi, D. Loreggia, G. Massone


Fringe Tracker Design for VLTI Spectro-Imager

Issue: 1.0
Date: 9-11-2007

	Fringe Tracker Design for VLTI Spectro-Imager	Rep: 87/2007 Issue: 1.0 Date: 9-11-2007
---	--	---

Contents

1	Applicable and Reference Documents	4
1.1	Applicable Documents	4
1.2	Reference Documents	5
2	Acronyms	6
3	Scope	9
4	Introduction	9
5	High level operational modes	10
6	Instrument description	11
6.1	Atmospheric Dispersion Compensation	12
6.2	Beam combination	15
6.3	Spatial filtering	16
6.4	Spectral dispersion	18
6.5	Signal detection	19
6.5.1	Measurement algorithms	22
6.6	Scaling the system to 4 or 8 beams	23
6.6.1	VSI4 phase: 4-beam configuration	24
6.6.2	VSI8-Hyb/AT phase: 8-beam configuration	25
7	Definition of the interfaces	26
7.0.3	Alignment and cophasing	26
7.1	SW interfaces	27
7.2	Mitigation of non-common OPD noise	27
8	Control system requirements	27
8.1	ADC control	27
8.2	OPD modulation	28
8.3	Fibre injection	28
8.4	Detector	28
8.5	OPD control loop	29
8.6	OPD correction	29
9	System performance	29
9.1	Optical throughput budget	30
9.2	System visibility	31
9.3	Read noise	32
9.4	Thermal background	33

	Fringe Tracker Design for VLTI Spectro-Imager	Rep: 87/2007 Issue: 1.0 Date: 9-11-2007
---	--	---

9.5 SNR calculation 33



Fringe Tracker Design for VLTI Spectro-Imager


Rep: 87/2007
Issue: 1.0
Date: 9-11-2007

1 Applicable and Reference Documents

1.1 Applicable Documents

No.	Document title	Reference	Issue	Date
AD1	Technical Requirements and Specifications for the Phase A Study of the VSI Instrument	VLT-SPE-ESO-15870-0001	1.0	24.05.2006
AD2	Interface Control Document between VLTI and its Instruments	VLT-ICD-ESO-15000-1826	4.0	11.08.2005
AD3	Requirements for Safety Analysis	VLT-TRE-ESO-00000-0467	1.0	27.07.1993
AD4	General safety requirements for scientific instruments	VLT-SPE-ESO-10000-0017	2.0	16.09.1992
AD5	Acceptance procedure electrical safety and EMC	VLT-VER-ESO-10000-0958	2.0	01.03.1996
AD6	Electromagnetic compatibility and power quality specifications part 1: electromagnetic environment of the VLT observatory and EMC levels of the power system	VLT-SPE-ESO-10000-0002	2.0	11.03.1992
AD7	Electromagnetic compatibility and power quality specifications, part 2: electromagnetic disturbance emission and immunity limits of electric and electronic equipment	VLT-SPE-ESO-10000-0003	1.0	05.09.1992


continued on next page

	Fringe Tracker Design for VLTI Spectro-Imager	Rep: 87/2007 Issue: 1.0 Date: 9-11-2007
---	--	---

<i>continued from previous page</i>				
No.	Document title	Reference	Issue	Date
AD8	VLT electronic design specifications	VLT-SPE-ESO-10000-0015	5.0	06.03.01
AD9	VLT Environmental specifications	VLT-SPE-ESO-10000-0004	6.0	12.11.1997

1.2 Reference Documents

No.	Document title	Reference	Issue	Date
RD1	VLTI Spectro-Imager — Technical Proposal for a second generation VLTI instrument	VSI-PRO-001	1.0	30.01.2006
RD2	VLTI Spectro-Imager — Science Cases	VSI-PRO-002	1.0	30.01.2006
RD3	VLTI Spectro-Imager — Letters of Intent from the Institutes of the VSI consortium	VSI-PRO-003	1.0	30.01.2006
RD4	Managment Plan	VLT-SPE-VSI-15870-4338	1.0	30.06.2007
RD5	System Design	VLT-SPE-VSI-15870-4339	1.0	30.06.2007
RD6	Control System Design	VLT-SPE-VSI-15870-4344	1.0	30.06.2007
RD7	Detector System	VLT-SPE-VSI-15870-4346	1.0	30.06.2007
RD8	Assembly Integration Test Plan	VLT-PLA-15870-0002	1.0	30.06.2007

	Fringe Tracker Design for VLTI Spectro-Imager	Rep: 87/2007 Issue: 1.0 Date: 9-11-2007
---	--	---

2 Acronyms

AD Applicable Document

ADC Atmospheric Dispersion Compensation

AGN Active Galactic Nucleus

ALMA Atacama Large Millimeter Array

AMBER Astronomical Multi-BEam Recombiner

AO Adaptive Optics

AT Auxiliary telescopes (1.8m)

AU Astronomical Unit

BLR Broad-Line Regions

BOBCAT Bulk Optics Beam Combiner And Tracker, project of an instrument of second generation.

CHARA Center for High Angular Resolution Astronomy

CRIRES Cryogenic High-Resolution IR Echelle Spectrometer

EGP Extra-Solar Giant Planet

FINITO First generation fringe tracking unit

FOV Field of View

FT Fringe Tracker

FTE Full Time Equivalent

FWHM Full Width at Half Maximum

GRAVITY One of the proposed concepts for the 2ng generation VLTI instrument


GD Group delay

HST Hubble Space Telescope

ICS Instrument Control Software

IONIC Integrated Optics Near-Infrared Combiner

IOTA Infrared Optical Telescope Array

	Fringe Tracker Design for VLTI Spectro-Imager	Rep: 87/2007 Issue: 1.0 Date: 9-11-2007
---	--	---

IR Infra-Red

JMMC Jean-Marie Mariotti Center

KI Keck Interferometer

LCU Local control unit

MATISSE One of the proposed concepts for the 2^{ng} generation VLTI instrument

MHD Magneto-Hydro-Dynamics

MIDI MID-Infrared VLTI first generation instrument

MOS Multi-Object Spectroscopy

MROI Magdalena Ridge Observatory Interferometer

MS Main Sequence

NACO NAOS/CONICA

NAOS Nasmyth Adaptive Optics System

NDRO Non-Destructive Readout

NGST New Generation Space Telescope

NIR Near Infrared

NPOI Navy Prototype Optical Interferometer

OPD Optical Path Difference

PdBI Plateau de Bure Interferometer

PMS Pre-Main Sequence

PNe Planetary Nebulae

PRIMA Phase-Reference Imaging and Micro-arcsecond Astrometry

PSF Point Spread Function

RD Reference Document

RON Readout Noise

RV Radial Velocity

SINFONI Spectrograph for INtegral Field Observations in the Near Infrared



Fringe Tracker Design for VLTI Spectro-Imager

Rep: 87/2007
Issue: 1.0
Date: 9-11-2007

SNR Signal to Noise Ratio

SR Strehl Ratio

STS Star Telescope Separator

TBC To Be Confirmed

TBD To Be Defined

TBW To Be Written

UT Unit Telescope (8m)

VINCI VLT Interferometer Near-Infrared Commissioning Instrument

VITRUV Not an acronym. Project of an instrument of second generation.

VLT Very Large Telescope

VLTI Very Large Telescope Interferometer

VSI VLTI Spectro-Imager



Fringe Tracker Design for VLTI Spectro-Imager

Rep: 87/2007
Issue: 1.0
Date: 9-11-2007

3 Scope

The document describes the Fringe Tracker design of VLTI Spectro-Imager proposed for the ESO call for phase A studies of 2nd generation VLTI instrumentation.

4 Introduction

VLTI Spectro Imager (VSI) is proposed as a second-generation VLTI instrument providing the ESO community with spectrally-resolved near-infrared images at angular resolutions down to 1.1 milliarcsecond and spectral resolutions up to $R = 12000$. Targets as faint as $K = 13$ will be imaged without requiring a brighter reference object to be nearby; fainter targets can be accessed if a suitable reference is available. This unique combination of high-dynamic-range imaging at high angular resolution, high spectral resolution and 100% sky coverage for a range of targets enables a scientific programme which will serve a broad user community within ESO and at the same time provide the opportunity for breakthroughs in many areas at the forefront of astrophysics.

A critical feature of VSI is that it will provide these new capabilities while using technologies which have been extensively tested in the past and while requiring little in terms of new infrastructure on the VLTI. At the same time, VSI will be able to make maximum use of new infrastructure as it becomes available. VSI provides the VLTI with an instrument capable of combining up to 8 telescopes, enabling rapid imaging through measurement of up to 28 visibilities in every wavelength channel within a few minutes. Operations with less than 8 telescopes is the scope of the first phases of VSI even it requires more VLTI configurations to obtain the same image quality.

Three development phases are foreseen: VSI4 combining 4 telescopes (UTs or ATs), VSI6 combining 6 telescopes (4UTS+2ATs or 4ATs+2UTS and eventually 6ATs) and ultimately, in the longer term if it happens, VSI8 combining 8 telescopes (4UTs+4ATs or eventually 8ATs). The current studies are focused on a 4-telescope version with an upgrade to a 6-telescope one. The instrument contains its own fringe tracker and wavefront control in order to reduce the constraints on the VLTI infrastructure and maximize the scientific return.

The high level specifications of the instrument are derived from a detailed science cases based on the capability to make milliarcsecond-resolution images for the first time of a wide range of targets including:

- Probing the initial conditions for planet formation in the AU-scale environments of young stars;
- Imaging convective cells and other phenomena on the surfaces of stars;
- Mapping the chemical and physical environments of evolved stars, stellar remnants and stellar winds;
- Disentangling the central regions of active galactic nuclei and supermassive black holes

This has led to an instrument concept consisting of:



Fringe Tracker Design for VLTI Spectro-Imager

Rep: 87/2007
Issue: 1.0
Date: 9-11-2007

- Integrated optics multi-way beam combiners providing high-stability visibility and closurephase measurements on multiple baselines;
- A cooled spectrograph providing resolutions of between $R = 100$ and $R = 12000$ over the J, H, or K bands;
- An integrated high-sensitivity switchable H/K fringe tracker capable of real-time cophasing or coherencing of the beams from faint or resolved sources;
- Hardware and software to enable the instrument to be aligned, calibrated and operated with minimum staff overhead;

As a whole, VSI is designed to feature 4 main components: the Science Instrument (SI), the Fringe Tracker (FT), the Common Path (CP) and the Calibration and Alignment Tools (CAT). The Optics design of the Science Instrument (see Optics Design document, RD10) features beam combination using single mode fibers, an Integrated Optics (IO) chip and 4 spectral resolutions through a cooled spectrograph. The Common Path includes low-order adaptive optics aimed at only tip-tilt corrections. VSI also features an internal fringe tracker. These servoloop systems relax the constraints on the VLTI interfaces by allowing to servo optical path length differences and optimize the fiber injection of the input beams to the required level. An internal optical switchyard allows the operator to choose the best configuration of the VLTI co-phasing scheme in order to perform phase bootstrapping for the longest baseline on over-resolved objects. In the next sections, we present the design of the Fringe Tracker unit which complies with the mechanic and functional requirements of VSI: Sect. 5 gives a brief description of the main functions the FT has to provide; the description of the instrument design is given Sect. 6, together with the implementation of the its basic functions; the fundamental operations required to properly put the FT in operation in VSI, and the involved interfaces toward the Science Instrument and the Common Path assembly are discussed in Sect. 7; the specification of control functions of the FT are summarised in Sect. 8; finally, the computation of the expected optical performance and the ensuing operational limiting magnitudes of the proposed design are shown in details in Sect. 9.

5 High level operational modes

VSI is required to be equipped with its own internal Fringe Tracker (FT), which must be capable of co-phasing at least four telescopes, with a possible extension to six and eight telescope array. The VSI fringe tracker has to estimate and correct both phase and group delay errors, meaning short ($\sim \lambda$ or less) or long ($\sim \lambda$ to 10λ) range piston fluctuations induced by atmospheric turbulence, on a number of baselines (e.g. at least 5 in six beam combination case) suited to stabilise the whole telescope array.

The visibility of the source and the loss of contrast in the instrument are essential in the tracking strategy; the fringe contrast and the related SNR on the fringe phase are used to evaluate delay errors which must be sent to the control system in order to produce data quality information. The FT will measure fringe parameters in H or K band alternatively, making use of dispersed fringes over at least three sub-bands, for a proper implementation of both phase and group delay measurements.



Fringe Tracker Design for VLTI Spectro-Imager

Rep: 87/2007
Issue: 1.0
Date: 9-11-2007

In order to fulfill the science goals of high-SNR, high-spectral-resolution imaging, the VSI FT has to provide the following functional modes.

Fringe Acquisition: the FT searches for fringes, i.e. locates the fringe envelope, by scanning a relatively large OPD range (e.g. $100 - 200 \mu\text{m}$ about the nominal zero OPD position defined by the VLTI Delay lines blind tracking), along the available baselines. It is preferable to equip the instrument with its own OPD scan device, in order to allow FT to implement autonomously the fringe acquisition by either a continuous or stepped scan together with a group-delay algorithm to efficiently detect the presence of fringes. However, because of the potentially large uncertainty on the nominal zero-OPD location, OPD scan is likely to require to explore longer range and eventually to complement the internal scan with an ad-hoc motion of VLTI Delay Lines, e.g. by superposing a step-wise motion to the nominal blind tracking. The appropriate fringe acquisition strategy shall be defined with ESO.

Hardware cophasing: the OPD error, associated to fringe phase fluctuations, is measured and fed back, in real time and at high speed, either to the OPD compensator internal to VSI or to the VLTI Delay Lines, in order to stabilize baselines down to a few tenths of working wavelength (e.g. $\lambda/20$), thus allowing on-chip integration on the scientific instrument over several atmospheric coherence times.

Hardware coherencing: the GD error, i.e. the white light fringe position variation, is compensated in real time at lower speed, to keep stable fringes within a fraction of the coherence length (e.g. maintaining fringes in the coherence envelope with 1λ accuracy) and the fringe contrast to adequate levels to integrate fringes incoherently over minutes.

Fringe recording: besides their specific usage in OPD control, the FT data - e.g. phase error, GD estimate and visibilities related to the controlled baselines - are time tagged and archived in order to allow post-hoc (off line) monitoring of the observation quality, as well as calibration or correction of science data: this is also related to implementation of the software cophasing tracking or coherencing modes.

6 Instrument description

The Fringe Tracker is conceived as a number of separate functional units that fit together and within the VSI as a whole as shown in Figure 1. The light beams from the VLTI telescopes enter the VSI common path assembly, then the light is split between the science instrument and the fringe tracker, typically using dichroics that select either H or K for the fringe tracker. The common path system performs several functions on VLTI beams, and make them available to the VSI subsystems, i.e. the Fringe Tracker and the Scientific instrument, in position and shape suited for the VSI operations:

1. Switchyard performs different tasks:
 - Allow the mapping between the beam arrangement from the VLTI and the input of the beam combining optics, and eventually permute entering beams to make nearest-neighbour telescopes within the VLTI appear as nearest-neighbour beams at the input of VSI.



Fringe Tracker Design for VLTI Spectro-Imager

Rep: 87/2007
Issue: 1.0
Date: 9-11-2007

- Adjust the transverse positions of the entering beams to be matched to that expected by the FT beam combiner.
 - Allow the tilts of the beams entering the FT combiner to be matched with the tilts expected by the beam combiner for maximum fringe contrast and maximum coupling to the FT detector.
2. OPD correction unit stabilises the VSI optical path against the piston jitter due to atmospheric turbulence, which is measured and compensated by the Fringe Tracker
 3. Tip/Tilt correction recovers the quality of beam wavefront under the control of the internal Imaging System; as demonstrated in previous experiences, the wavefront quality is degraded, in spite of the telescope adaptive correction, because of local unexpected and uncontrolled turbulence within VLTI tunnels.
 4. Wavelength selection is achieved by dichroics, which split photons according to the wanted observing wavelength on the SI and operational wavelength of the FT.
 5. Calibration Alignment Tool (CAT) provides reference source for calibration purpose as well as for supporting the internal alignment of the VSI arms, during integration and set-up phases. The light injection occurs at the position assumed as zero phase reference plane of VSI.
 6. Atmospheric Dispersion Compensation removes the differential effects - optical path mismatch and angular shift of source apparent position - of atmospheric dispersion due to the different operating wavelength of the Fringe Tracker with respect to the observing wavelength of the Scientific Instrument.

Within the Fringe Tracker, the beam combination occurs in pairwise between all the incoming beams; besides the nearest-neighbour pairs (i.e. $N-1$ with N input beams), the two extreme beams - beam #1 and beam # N - are also brought to superposition, so as to allow the usage of N baselines instead of the minimum $N-1$, and thus linking in a ring all the telescopes feeding the interferometer. The combined signals are spatially filtered by injection into optical fibres, which, in turn, transport the signal into a cryogenic dewar. Inside the dewar, a cryogenic spectrograph allows fringes to be measured simultaneously in a suitable number of adjacent spectral channels covering one complete spectral band, either H or K. The spectrograph light falls on the detector, the output of which is digitised and fed to the OPD servo, which executes the FT algorithms, computes the OPD error on all the measured baselines and feeds error signals to the internal fast OPD corrector and the VLTI delay lines.

6.1 Atmospheric Dispersion Compensation

During observations, since the fringe tracker and the scientific instrument operate in different wavelengths, over a field at a given zenithal distance, there is a mismatch between their respective zero-OPD, due to the different evolution of the optical path along the common air column, as well as a different apparent position on the sky associated to differential refraction. To compensate the

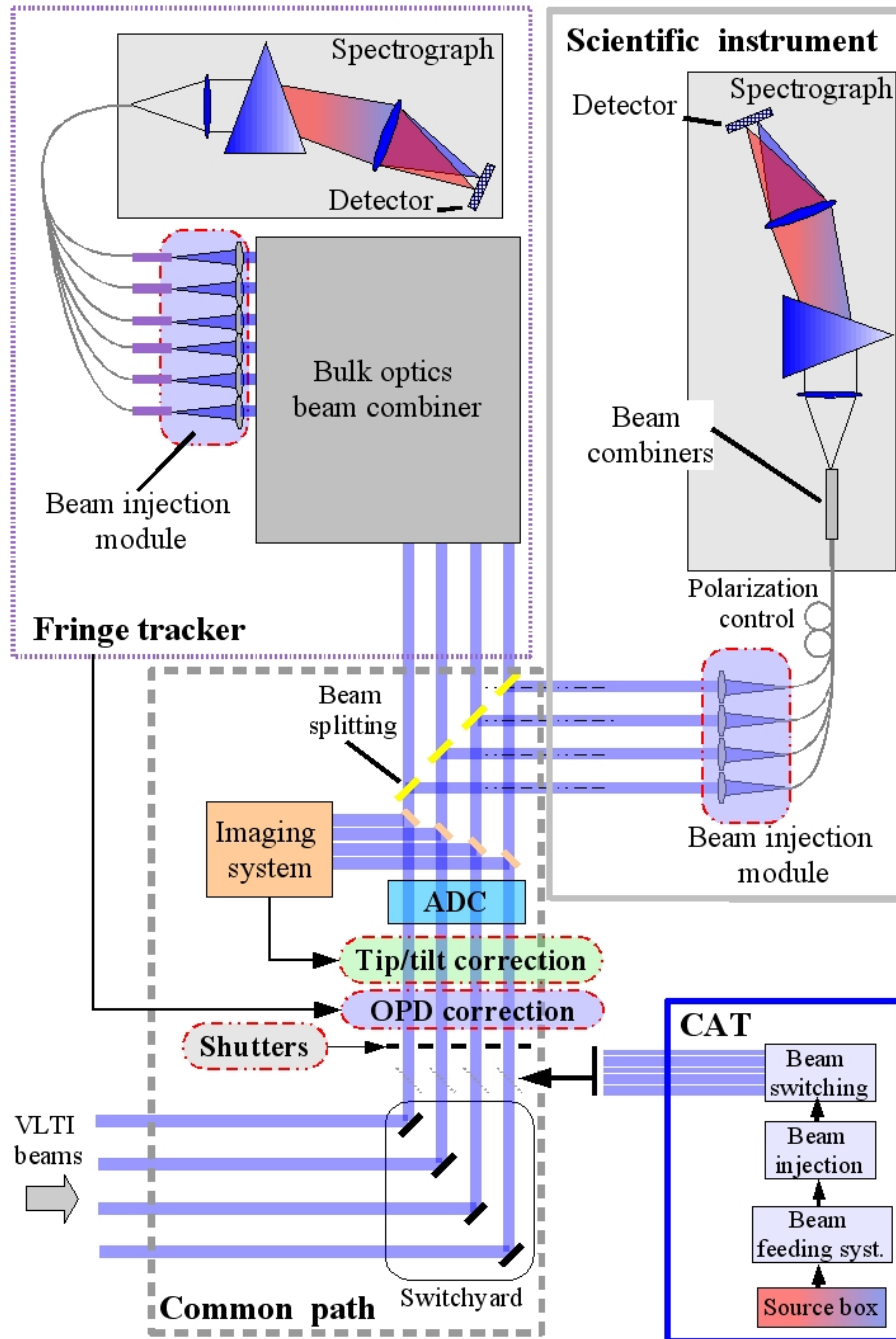


Figure 1: VSI system conceptual diagram.

chromatic mismatch, an Atmospheric Dispersion Corrector is required, operating on both components: the longitudinal correction introduces an appropriate OPD variation, and the transversal correction compensates the separation between the observing directions on the sky.

The effects of atmospheric dispersion on shift of the zero-OPD position and on the beam direction when observing at different wavelengths, because of the change in refractive index, depend upon the wavelength separation, the position on the sky (zenithal distance) and the weather conditions. The values applicable to the FT can be derived from the figure below (Figure 2), where the differential refraction is shown as a function of wavelength in standard weather conditions and at high zenithal distance (60 degree): the differences are computed using the value at $1.6 \mu\text{m}$ as a reference; the refraction index and refraction constant are taken from Allen, "Astrophysical Quantities". An angular separation of $0''.4$ between the apparent positions in J and K, when observing at high zenith angle with a 100m projected baseline, is associated to a shift of zero-OPD position of the order of $200 \mu\text{m}$. The angular displacement in laboratory units can be deduced taking into account the beam compression factor of 444 between the 8m UT aperture and the 18 mm VLTI beam diameter, corresponding to an equal angular magnification factor, so the required regulation stroke in the lab is less than $\pm 1 \text{ mrad}$. A fully performing ADC device, e.g. translating and rotating prisms,

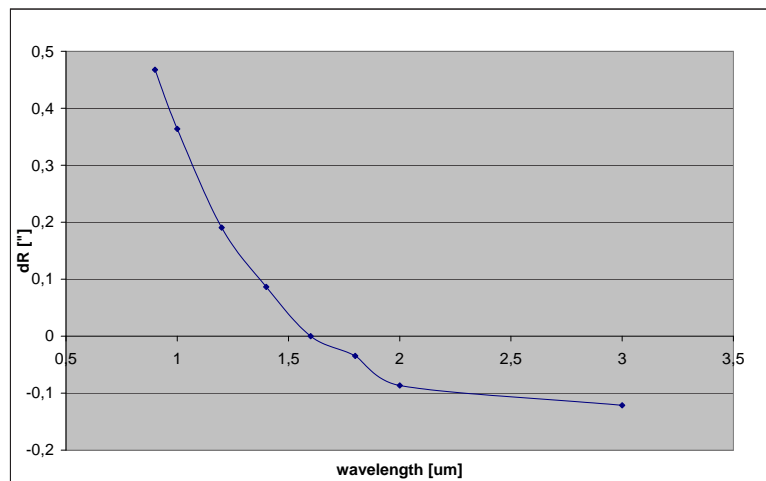



Figure 2: Differential refraction vs wavelength: at 60 degree of zenithal distance (zero at $1.6 \mu\text{m}$).

claims for at least three degrees of freedom (DOF): translation for longitudinal component and two orthogonal rotations for transversal component.

The control requirements for the FT ADC devices could be limited to the sole longitudinal compensation, i.e. one linear degree of freedom, assuming to demand the compensation of the transversal component to other VSI common path component, e.g. switchyard stages.

However, the ADC solution with extended DOF is preferable, for it allows to also correct the

	Fringe Tracker Design for VLTI Spectro-Imager	Rep: 87/2007 Issue: 1.0 Date: 9-11-2007
---	--	---

intra-band dispersion effects, besides the inter-band ones for which an ADC with minimal DOF is sufficient.

In the current VSI design the ADC is deployed in the common path assembly, and its control is demanded to SI, which manages the observational configuration, e.g. wavelength selection, of the VSI as a whole, according to the astronomical observations to carry out. The figure below shows the foreseen VSI wavelength selection arrangement, which includes the ADC device; more details are provided in the system design document(RD5).



Figure 3: VSI wavelength selection configuration: H band to FT (left), K band to FT(right)

6.2 Beam combination

The layout of the optics for the beam combiner, for the six beam configuration case - adopted baseline configuration for the FT, is shown in Figure 4. Light beams entering the combiner from the left are split into two parts by beam-splitters and each half is combined with the light from the nearest-neighbour beam to form fringes. The minimum redundancy, i.e. the telescope ring closure, is obtained by superposing beams 1 and 6, whose combination needs additional optics component: one folding mirror M3 and one optical path delay system DL. The planar layout, beam angles, as well as the common beam splitting and beam combination arrangement, are preserved; beam 6 is folded by mirror M3 towards the position of beam 1 into the beam combiner, and the balance of the optical path between the two beams is achieved by introducing an internal delay through the DL device.

All the combination pairs are symmetric, so that the measurements are potentially achievable at equivalent SNR along all the controlled baselines.

Hereafter, such a combination scheme will be referred to as the **Planar Minimum Redundancy Combiner (PMRC)**.



Fringe Tracker Design for VLTI Spectro-Imager

Rep: 87/2007
Issue: 1.0
Date: 9-11-2007

From the beam-combiner emerges pairs of complementary outputs, 180 degrees out of phase (the so-called "AC" pair of measurements).

The geometry of the layout has been arranged to allow low angles of incidence, order of 30 degrees, onto the beamsplitters. This allows high-efficiency dielectric beamsplitter coatings to be used, and also means that the amplitude and phase differences between the S and P polarisations are small (typically less than 1% in amplitude). Thus unpolarised fringes can be formed with little loss in fringe contrast. Alternatively it is possible to insert quarter-wave plates between the first set of beam-splitters and the second set and a Wollaston prism into the spectrograph, and produce quadrature fringes in the two polarisations, i.e. the A and B fringe signals in the S and P polarisations respectively in the outputs on one side of the beamsplitter and the C and D signals in the outputs on the other side of the beamsplitter. This latter option is not considered further in any detail here, i.e. we assume that fringes are formed in unpolarised light. Instead we assume that the quadrature outputs are measured using temporal modulation of the fringe phase. To do this, the mirrors in either Mirror Bank 1 are mounted on piezoelectric actuators and their positions are stepped by a quarter of a wavelength (at the central wavelength of the working band) in the middle of every exposure. The detector readout is synchronised with the stepping of the piezos so that the detector senses from one side of the beamsplitters first phase A then phase B signals, while from the other side phase C then D fringe signals. Stepping the piezos rather than scanning them means that the fringes are not "smeared" during the detector integration time: this can cause a 10% loss in visibility when using a linear scan instead of a stepped scan.

The size of this optical layout is a strong function of the beam-to-beam lateral spacing. The size shown in the diagram (Figure 4) is relative to "beam pitch" of 35 mm; the whole footprint has been minimised assuming monolithic mounts for beamsplitters and mirrors.

The chief advantages of this optical scheme are:

1. The telescopes are closed in a ring and all baselines are measured with minimum dilution of light
2. Minimum number of surfaces to introduce photon losses or wavefront distortion: each beam sees a total of two beamsplitters plus one reflection between the FT entrance and the dewar coupling optics
3. High-efficiency beamsplitter coatings can be used because of the low angles of incidence
4. The alignment of the system is straightforward, being a simple pairwise scheme
5. The system can be easily scaled for any number of beams

6.3 Spatial filtering

The beam combiner outputs are spatially filtered by focusing them onto fibres, which carry the interferometric spots directly into the cryostat, where they are sensed by a single array detector. After combination, fibres are not requested to operate in single mode, as there is no need to keep on preserving the phase signal; however, the usage of mono mode fibres appears justified for at least the following reasons:

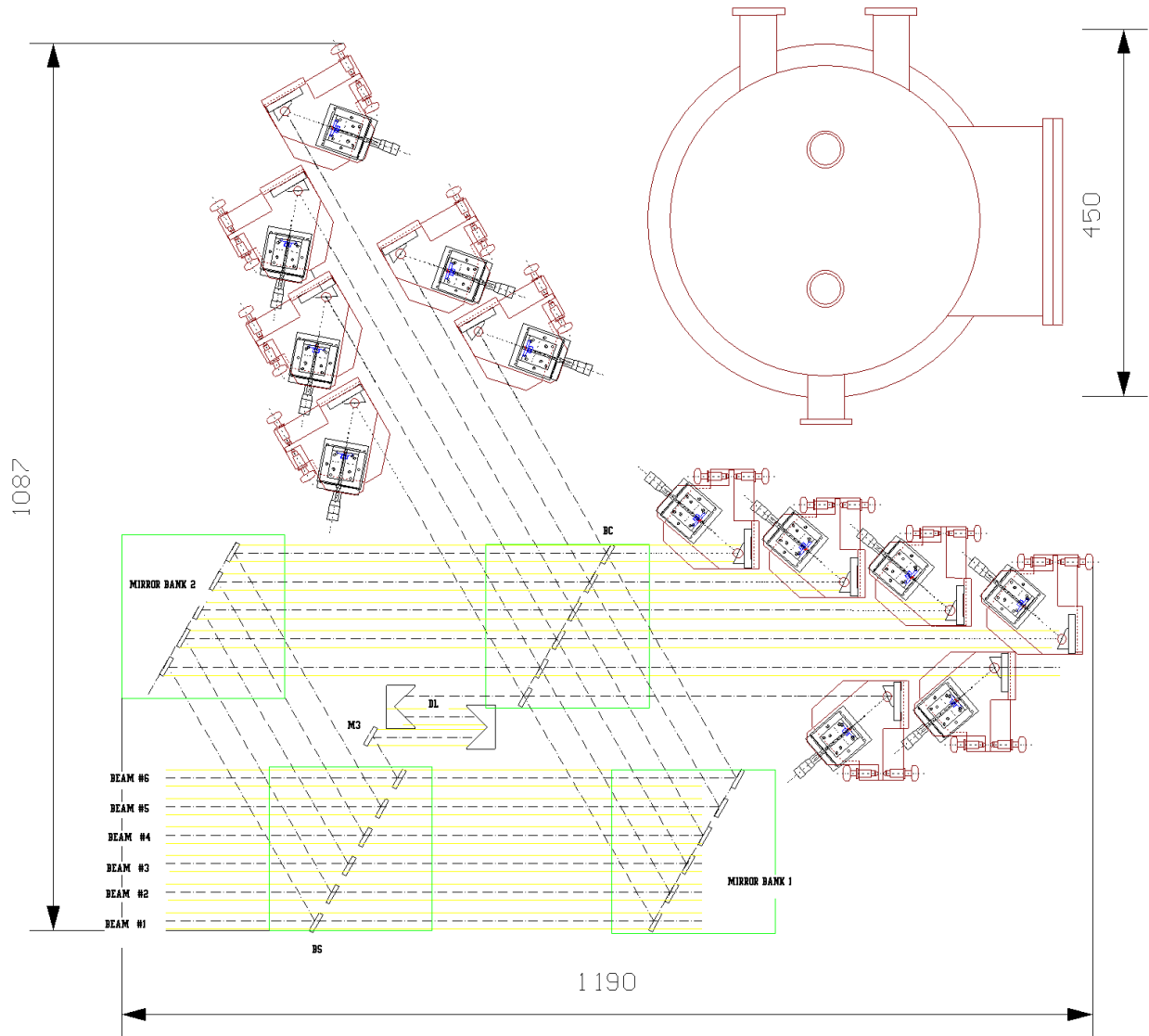


Figure 4: Fringe tracker's beam combiner layout

1. ease the signal re-imaging and mapping onto detector's pixels
2. reduce the thermal background.



Fringe Tracker Design for VLTI Spectro-Imager

Rep: 87/2007
Issue: 1.0
Date: 9-11-2007

3. filter out the residual wave front corrugation - left by adaptive optic correction - by focusing/matching the PSF central lobe onto the fibre core.

Moreover as experienced in previous experiences for PRIMA FSU, employing cold fibres and optics, instead of standard warm, has proven to further decrease the external background of at least one order of magnitude.

The fibre injection optics design (Figure 5) shares the solution in use in the SI: a parabolic mirror, 25 mm in size, focuses the light onto the fibre, which is kept in position by a stage featuring at least X/Y degrees of freedom for fine tuning; focus position is not reckoned so critical to require an additional degree of regulation. As the injection adjustment is expected to occur routinely, the remote control of the fibre positioning is highly recommended, so as to avoid frequent human intervention in lab; then the fiber positioners are requested to be equipped with motors.

Measurements in two bands require in principle two sets of fibre bundles (each tailored for each operating band, H and K). The use of a single mono-mode K fibre for both operational bands appears also feasible and compatible with expected performances; the approach also simplifies greatly the relay optic design, and eases the implementation of switching between the working spectral bands. The partial multi mode behaviour in H band of a single-mode K fibre can possibly introduce fluctuations on the lateral deviation of the H beam at fibres' outputs. The analysis carried out so far shows that the resulting shift of signal spots onto the detectors looks marginal and acceptable; furthermore, the effect can be partially compensated or controlled by accurate design of the camera spectrograph and of the fibre positioning in front to the detector, e.g. linear arrangement instead of bi-dimensional fibre array.

The common H+K fibre solution is assumed as baseline configuration of the spatial filtering function; the distortion effects in H band will be further and deeper investigated during the next design phase.

6.4 Spectral dispersion

Inside the dewar, fibres are properly aligned in front of a dispersive optics, e.g. doublets + prism, which spectrally disperses spots over few, 3 to 5, pixels, so as to allow the implementation of co-phasing and coherencing operational modes. The order of spectral dispersion needs careful assessment to make the tracking algorithm sensitive and reliable: the higher the resolution is, potentially the more sensitive the tracking algorithm is to fringe smearing or to large fringe jump; but with less photons in every spectral element, the fringe measurements are likely accomplished at reduced SNR.

Provisional analysis (see VSI report VSI-SYS-004), derived from equivalent and already applied implementation (i.e. PRIMA FSU), demonstrates how splitting the working band, either H or K, in five sub-bands makes available just three central wavelengths for efficient usage in the measurements (effective wavelengths at 2.02, 2.16 and 2.32 μm for the K band case, with spectral resolution 35, 26 and 32 respectively). The signal is actually concentrated mostly in the three central sub-bands, and the nearby pixels receive a marginal fraction of the signal, which shall be further minimised during design optimisation. The three wavelength approach is the baseline solution selected for the VSI FT operations, it allows a good trade-off between algorithm robustness and control loop bandwidth:

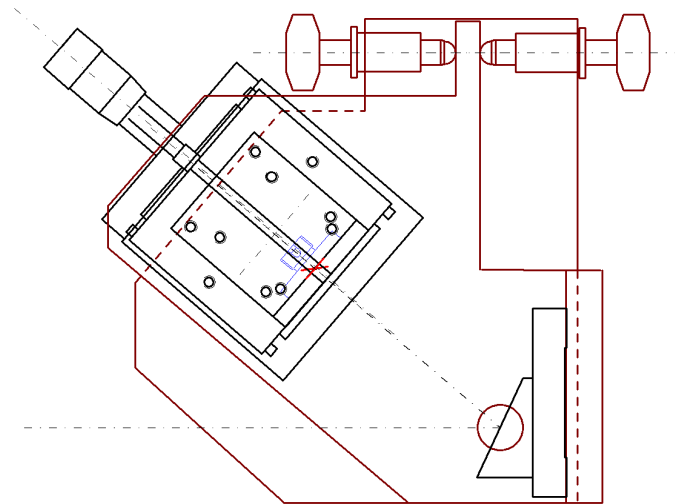


Figure 5: Fibre injection optics assembly

adequate photon distribution among three bands allows measurements at high SNR for accomplishing cophasing (from photons falling in the central band) and coherencing (from photons from lateral bands); reduced number of pixels ensures fast readout speed and high control bandwidth.

The optical design of the spectrograph (Figure ??) is simplified and requirements are relaxed if the fibres are arranged in uni-dimensional array and the dispersion occurs along a single row or column (see Sect. 6.5), selecting the faster scanning direction of the detector. The one dimensional design promises to be less expensive and less critical to construct and align.

Assuming to arrange the spectral dispersion such that the whole H+K band of each combiner output is continuously distributed over 6 pixels, i.e. 3 pixel dispersion per band, a complete scan for the six-telescope configuration requires to read at the most 72 detector pixels (twice for ABCD coding), and the working wavelength selection is achievable at pixel processing level, e.g. clocking only pixels associated to the working band, with no need of hardware reconfiguration inside and outside the dewar.

6.5 Signal detection

A feasible configuration for FT detection scheme is described below, assuming as design baseline the pair-wise beam combination with AC spatial modulation (extended with temporal step-wise modulation of the internal path for the implementation of ABCD measurement scheme), the provisional



Fringe Tracker Design for VLTI Spectro-Imager

Rep: 87/2007
Issue: 1.0
Date: 9-11-2007

spectral dispersion with 3 working wavelengths both for H (H1, H2 and H3) and K (K1, K2 and K3), and 6 feeding beams.

In its baseline configuration, the FT deals with 72 signal spots, just half of which needs to be read and processed for measurements in a single band. Signals are properly mapped and processed, according to detector's pixel architecture, in order to allow measurements at high SNR and high speed.

HAWAII-1 detector from Teledyne Imaging Sensors (former Rockwell) is the sensors selected for the VSI FT; the pixel array (1024x1024 pixels, 18.5 μm in size) is arranged in 4 quadrants - 512x512 pixels in size, with independent outputs. The linear, one dimensional configuration of the spectrograph proposed above (Sect. 6.4) is mapped onto the quadrant architecture by focusing phase A and phase C signals onto two adjacent quadrants, i.e. 6 spectra per quadrant; spectra are distributed along a common pixel row, with a horizontal inter-spectra guard-gap, within a single quadrant, of few pixels, e.g. 3 pixel wide. The complete scan involves 2 detector outputs and 36 pixels per output plus some reference pixels.

Reference pixel values (for effective data processing, e.g. bias subtraction) can be either taken from some -one or two- of the inter-band pixels, with negligible increase in readout time of one or two pixel time, or acquired in parallel from spare outputs with no increase in readout time.

As the detection map makes available the H and K spectra simultaneously (one after the other through a common amplifier), operating wavelength selection doesn't imply any change in hardware, and it is accomplishable at pixel processing level, either at detector control level by clocking just the window of pixels of the selected band or at LCU level by processing pixel data associated to the band of interest. Tracking algorithm performance are set by sensors intrinsic features, as well as signal processing techniques in use.

Measurement SNR definitively depends on the adopted detector readout mode:

CDS Mode: In conventional Correlated Double Sampling (CDS) mode, the HAWAII-1 elementary readout noise (RON) is of 15 electrons rms at the maximum pixel sampling rate of 500KHz (see VSI Detector System document RD7).

NDRO Mode: Non-Destructive Readout (NDRO) technique is associated to multiple sampling of the video signal along the detector integration ramp and to the linear fit of the collected signal points. If applied with N number of samples, the technique reduces the effective RON by a factor of $\sqrt{\frac{6(n-1)}{n(n+1)}}$ with respect to the figure of the basic CDS scheme; with order of 100 samples, the effective RON, potentially achievable by HAWAII-1, is lower than 4-5 electrons. Depending on the number of samples involved, NDRO approach is eventually applicable to the FT in quite good atmospheric condition regimes (e.g. coherence time longer than 2 ms).

Concerning control loop bandwidth, a single readout sequence for the AC coding takes 72 microseconds, to read 72 pixels (H+K dispersed bands) equally divided between two parallel outputs; CDS mode needs twice those times, i.e. 144 μs at the maximum sampling rate HAWAII-1 allows. Allocating a convenient overhead for skipping the pixels of inter-band gap (about 1 μs per gap, applicable only to the quadrant detector) and for dead time (e.g. one frame time, order of 100 μs) for stepping the internal optical path, the maximum rate sustainable for a complete set of "ABCD" readings, i.e. the fringe tracking control loop bandwidth, is realistically close to 2KHz, which rises

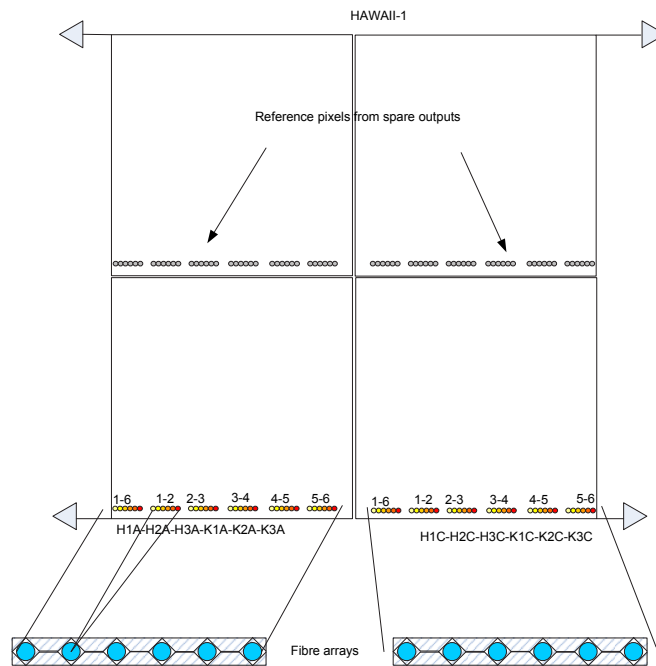


Figure 6: FT detection scheme by HAWAII-1 detector

to 2.8KHz if the readout involves only the spectral channels associated to the selected working wavelength, i.e 18 pixels per output instead of 36.



Fringe Tracker Design for VLTI Spectro-Imager

Rep: 87/2007
Issue: 1.0
Date: 9-11-2007

The performance is well compatible with reasonable values of the fringe coherence time, quoted as $4ms$ in H and $6ms$ in K; it allows for a fringe sampling rate (equivalent to the 2-step modulation rate of the piezo modulator of the FT beam combiner) from eight to twelve times faster than the expected atmospheric fringe jitter, ultimately set by the weather conditions.

6.5.1 Measurement algorithms

The goal of the VSI FT is the determination in real time of the information for fringe tracking on the scientific combiner. Depending on the desired overall operation mode, e.g. OPD (phase) tracking or GD tracking, and on the possible implementation of robust control algorithms, the required data are different and possibly on different time scales.

Hereafter, we describe the baseline algorithms considered for OPD and GD estimation and we provide some implementation considerations. We recall that the proposed FT concept generates the complementary outputs from pair-wise combination of the six input VLTI beams according to a nearest-neighbour scheme. The combined signals are dispersed to generate three or four spectral channels in either H or K band (to be optimised in the detailed design). Temporal modulation is used for either normal operation (short range, e.g. a fraction of wavelength) or for special operating modes (intermediate range, up to a few fringes), e.g. technical verifications. The parameters estimated from the FT detector values will be, for each combination: the OPD; the GD; the (squared) visibility; a photometric indicator related to the overall detected flux in each sub-band; a few parameters estimated from the measurements as exposure quality indicators, e.g. the relative discrepancy between the measurements and the current observation model (see below). The data will be logged on a suitable time scale (if required, after appropriate time filtering), and used in real time for fringe tracking within VSI. The option of data feedback to the ESO OPD Controller for DL monitoring or adjustment shall be discussed with ESO, if appropriate.

The pixel values derived by detector readout according to the selected operating mode and time scale are to be processed to provide the desired elementary exposure measurements. This includes double or multiple correlated sampling, if used, dark and bias subtraction, where appropriate, and linearity correction. It is assumed that the pixel values are scaled to appropriate common reference units (e.g. photo-electrons or photons) before actual processing for estimation of the desired interferometric parameters.

The conceptual reference for the OPD estimate algorithm is the ABCD model, although this is not strictly valid for a detailed instrument description; anyway, the baseline is the achievement of four interferogram samples on distinct phase values, by usage of the complementary outputs and a short range OPD modulation within the FT. Hereafter, we will retain the terminology of A, B, C, D samples under the assumption that it is a namesake of the four subsequent samples. An elementary extension of the naïf ABCD algorithm is achieved by introduction of ad-hoc instrumental correction factors (e.g. custom phases) to be combined with the actual measurements to allow application of a generalised ABCD expression. The best performance in the simple case is dominated by the combined noise from photon statistics (due to the source and background fluxes), detector readout and external atmospheric turbulence (OPD and intensity fluctuations). It is computed by fitting the measurements to a detailed model taking into account the calibrated instrument response and the observing conditions, e.g. longitudinal and transversal dispersion. An implementation based



Fringe Tracker Design for VLTI Spectro-Imager

Rep: 87/2007
Issue: 1.0
Date: 9-11-2007

on the least square discrepancy approach is discussed e.g. in Gai et al. (SPIE workshop "New Frontiers in Stellar Interferometry" Glasgow (UK), 2004)]; for convenience, the numerical code can adopt an iterative procedure which can be shown equivalent to the Newton-Raphson algorithm. It should be noted that least square approaches are potentially affected by convergence problems in case of significant noise and above all of large variation of the measured system with respect to the model assumptions; this is the case e.g. for large fluctuations of phase and/or intensity on the input beams, as sometimes experienced in VLTI due to internal atmosphere or infrastructure sources (e.g. vibrations). The selection between least square and generalised ABCD algorithms will be performed according to criteria of both noise performance and robustness with respect to perturbations affecting the system response and not included in the measurement model. Also, the algorithms will generate not only the OPD estimate but also a validity flag, i.e. the relative discrepancy between the measured pixel values and the expectation from the current observation model. This will provide an indication of the possible variation of measurement conditions, leading to potential degradation of the science data (e.g. break of the tracking loop or large deviation from the nominal conditions). Optimal usage of such information (e.g. for optimisation of robust control algorithm and verification of system behaviour) shall be agreed within the VSI consortium and with ESO.

The OPD algorithm can be applied simultaneously on all spectral channels currently used by the FT, in order to provide an improvement in the noise performance thanks to the full photon flux. Besides, the phase variation over the spectral range is associated to the GD value, which can be derived taking advantage of such information. Again, the estimate may be derived from a simple model (e.g. of the expected profile of OPD variation over the band), or by direct fit of the pixel values to an overall measurement model. The above considerations of sensitivity to system variations and noise performance are applicable. The GD algorithm evaluation and selection will be done according to criteria of both noise performance and robustness with respect to external perturbations. The GD estimate is in any case more liable to errors associated to fringe jumps, either real or associated to false detections, due to the physical limitations of similar period of the interferograms in the spectral channels of a given band.

For several versions of the algorithms proposed above, an implementation was developed for the PRIMA FSU, therefore realistic estimates on the execution time, I/O and memory requirements are available. They shall be scaled to the conditions related to the current ESO compliant hardware and software. For the time being, no concern on processing needs has been evidenced.

6.6 Scaling the system to 4 or 8 beams

In the baseline configuration, the FT comes arranged to operate six telescopes and, because of the minimum redundancy solution in use for the beam combiner, to stabilise six baselines at once; the arrangement is compatible with the VSI configurations VSI6-Hyb and VSI-AT, described into memo VSI-SYS-035. Below, the development plans to adapt the FT for the other VSI operational phases are summarised: required interventions and refurbishment are considered for the initial VSI4 phase and for the further improvement to VSI8Hyb or VSI8-AT phase.

6.6.1 VSI4 phase: 4-beam configuration

Feeding beams Only the beams from 1 to 4, out of the six of the baseline configuration, are supplied with light.

ADC Two ADC devices, on beams #5 and #6, are redundant.

Beam combiner The MRC scheme is retained by moving back the folding mirror M3 (Figure 7) up to intercept beam#4, in order to bring it to superposition with beam#1. The internal delay line needs to be adjusted to balance the delay between the beam couple #1 and #4. The incidence angles remain unchanged.

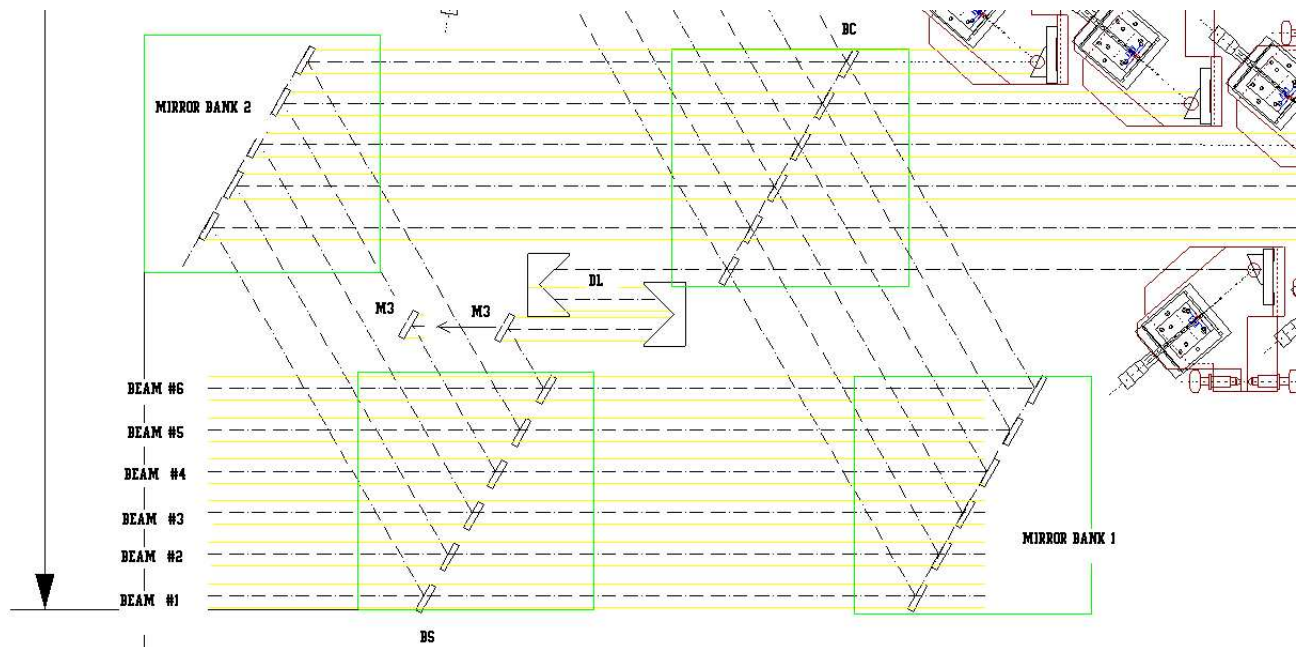


Figure 7: FT beam combiner: 4-beam configuration

Fibre injection Four fibre injection modules are redundant: two on each side of the beam combiner, namely the ones associated to the complementary outputs of the combination pairs 4-5 and 5-6.

Spectrograph No change is required.

Detection The sequence of the spectral dispersion on the detector is unaffected. The sensed pixels change from 72 to 48, evenly distributed among used detector outputs: The HAWAII-1



Fringe Tracker Design for VLTI Spectro-Imager

Rep: 87/2007
Issue: 1.0
Date: 9-11-2007

readout sequence is adapted by reconfiguring properly the detector controller, in order to read 24 pixels per output.

Footprint The FT space envelope is basically the same as for the six-beam arrangement.

Time scale Because of the reduced number of hardware interventions, confined to the set-up of the beam combiner, the adaptation to 4-beam configuration can be reasonably accomplished in a few day time scale, inclusive time for carrying out hardware checks and functional tests on the new arrangements.

6.6.2 VSI8-Hyb/AT phase: 8-beam configuration

Feeding beams Two extra beams are added below beam#1 of the six-beam baseline configuration.

ADC Two extra ADC devices are required.

Beam combiner The PMRC scheme can be retained, but all the components needs to be adapted in size and position to the 8-beam configuration. Monolithic mounts look still feasible, but deserve dedicated design phase.

Fibre injection Four extra fibres and injection modules are required, two on each side of the beam combiner.

Spectrograph A new design of 16-fibre array, compatible with the 8-beam combination and the detection scheme, is needed.

Detection The sequence of the spectral dispersion can be inherited from 6-beam configuration. The sensed pixels increase to 96 when combining 8 telescopes in the minimum redundancy configuration of the PMRC. The linear fibre array solution is still applicable. HAWAII-1 detector has to be properly clocked to handle 48 pixels per output.

Footprint The FT planar envelope is expected to increase accordingly to the number of beams, i.e. a factor 1.4 wider and longer.

Time scale One year design phase is reckoned suitable to identify and implement adequate solutions for optical components of the beam combiner, for the fibre array and its arrangement inside the cryostat.



Fringe Tracker Design for VLTI Spectro-Imager

Rep: 87/2007
Issue: 1.0
Date: 9-11-2007

7 Definition of the interfaces

The FT is designed to correct the piston fluctuations between the different telescopes so that the fringe pattern on the SI remains fixed during an integration. Therefore, it is of great importance that there are no significant OPD fluctuations between the FT and the SI. The input beams to VSI are separated as described in Sect. 6.2; a combination of mirrors and a dichroic component will define the beam transmitted to the FT. Any source of OPD fluctuations between the FT and SI will be in the non-common optical path and related optical components.

The fiber injection occurs after combination and therefore is not important on this respect. The opto/mechanical interfaces between FT and SI are limited to the VSI switchyard, the OPD correction module and the Calibration and alignment system. There is in addition to consider the footprint of the two systems and their accommodation on the available laboratory space. This aspect is covered in RD5.

The Calibration and alignment Tool (CAT) (described in RD5) will be a key system during integration and during normal operations. The mechanical stability of this module with respect to the SI and FT will directly influence the calibration and thus the final performance of the whole instrument.

7.0.3 Alignment and cophasing

This section includes the procedure of cophasing between SI and FT and of the whole VSI with the VLTI. This is in part described in VSI report vsi-sys-003.

First, the two instrument must be aligned between themselves and with respect to the VLTI beams; this will require the use of the alignment subsystem together with sky observations.

Then, both the SI and FT have to be cophased with respect of the CAT; this operation should be done during the system integration, and then as often as necessary, probably up to once at the start of each observing night. In any case, a translation with a few millimeter stroke should be sufficient.

The cophasing between FT and SI is needed at three levels:

- Correction of the differential longitudinal dispersion: in document "Analysis report of AMBER" (VLT-TRE-AMB-15830-0001) it is reported a compensation of about $100\mu\text{m}$ every few minutes. Therefore, a motorised translation will be needed, which could also be used to perform the initial cophasing between FT and SI. As explained in RD5, this function is performed by the OPD compensation module on the SI.
- Initial cophasing between FT and SI. As explained above, the OPD compensation module could perform this task.
- compensation of mechanical instabilities, induced for instance by microseismic events: if needed, one could use the motorized delay line described above, but these instabilities have to be made small and slow enough to allow meaningful measurements.



Fringe Tracker Design for VLTI Spectro-Imager

Rep: 87/2007
Issue: 1.0
Date: 9-11-2007

7.1 SW interfaces

Most of the interaction between FT and SI will occur at the software level. In particular we identify the following areas.

- Synchronization of OPD modulation; the modulation (necessary to perform the AC and BD measurements) must be started after fringe finding and synchronized with the detector read-out.
- Integration control, i.e. synchronisation with ICS in order to start the fringe finding procedure, and, when this is completed, send the OK status to the SI
- Quality control. Whenever the fringe signal is lost on one or more baselines, this information must be sent to the SI which could, for instance, interrupt the integration until a good fringe tracking is recovered.
- Related to the previous point, the FT could send information to the SI which could be used to operate a cold shutter (if implemented) in order to block the incident light during periods of low-quality signal or loss of fringe tracking.
- In case the ADC module introduces an OPD variation with respect to the FT, this must be compensated by the OPD compensation module

7.2 Mitigation of non-common OPD noise

The internal seeing in the laboratory will introduce an OPD drift which will be, for the common path component, corrected by the FT. However, the non-common path will be affected by differential OPD drifts that cannot be corrected and must be therefore assessed and minimized.

There is currently no estimate of what can be the amount of turbulence in the interferometric lab and how this could affect the measurements. This will have to be estimated in a later phase with laboratory experiments in Europe that can be representative of the conditions on Paranal. In any case, one should adopt all the measures that can be reasonably implemented in order to minimize such contribution. In addition to laboratory seeing, turbulence induced by thermal dissipation of electrical component on the VSI optical bench must be taken into account, together with acoustic noise and microseismic events. It must be investigated whether compliance with ESO requirements will be sufficient or, on the contrary, further steps are necessary to reach the design goals.

8 Control system requirements

The VSI control system is completely described in VSI Control System document (RD6) Hereafter, the main requirements for the functions to be implemented into FT subsystem, are summarised.

8.1 ADC control

Each entering beam is endowed with ADC device, featuring 3DOF;



Fringe Tracker Design for VLTI Spectro-Imager

Rep: 87/2007
Issue: 1.0
Date: 9-11-2007

Translation: stroke $200\ \mu\text{m}$, resolution $0.1\ \mu\text{m}$

Vertical tilt: stroke $\pm 1\text{mrad}$, resolution $10\ \mu\text{rad}$

Horizontal rotation: stroke $\pm 1\text{mrad}$, resolution $10\ \mu\text{rad}$

Update rate: $\leq 1\text{Hz}$

The 6-beam configuration claims for 18 controlled axis.

8.2 OPD modulation

The modulators will consist of mirrors mounted on piezo-electric actuators. There will likely be one modulator per baseline, but it may be possible to reduce the number of degrees of freedom with a monolithic actuator serving multiple baselines. The modulators are required to provide 1/4-wave steps at rates of between 20Hz and 2.8kHz. A total stroke of at least 1.1 microns is required, with a repeatability of better than 50nm for a given modulation waveform. However, it is advisable to extend the operational range of the modulator well beyond the requirement strictly necessary for the phase modulation. Extended modulation interval, say few hundred of micrometres with tens nanometres positional accuracy, could be useful for operating modes like fringe acquisition or calibration. Such performance are within the standard features of commercial devices.

The applicable performances to the piezo modulator are:

modulation range: $< 100\ \mu\text{m}$

modulation resolution: $0.01\ \mu\text{m}$

modulation rate: $< 3\text{kHz}$

8.3 Fibre injection

The fibre positioners shall permit the placement of the fibre end within the optical tolerances. As our past experience indicates that we can not trust on a stability of these systems within the required accuracy (due to several causes), a remote controlled actuator is foreseen.

More than two manual degrees of freedom are necessary for focus and tilt of the whole unit of off-axis mirror and fibre. The applicable requirements are:

X/Y remote controlled: $100\ \mu\text{m}$ range with $0.1\ \mu\text{m}$ resolution

Manual focus: $\pm 5\ \text{mm}$ with $2\ \mu\text{m}$ resolution

Angular adjustment: ± 1 degree with $0''.2 - 0''.4$ resolution

In 6-beam configuration, the FT needs 24 remote controlled axes plus 24 manual regulators.

8.4 Detector

The HAWAII-1 detector is operated by the ESO standard detector controller and delivered software.



Fringe Tracker Design for VLTI Spectro-Imager

Rep: 87/2007
Issue: 1.0
Date: 9-11-2007

8.5 OPD control loop

The control loop reads in the pixel information from the detector subsystem, derives a set of OPD correction signals for each telescope (one degree of freedom can remain fixed because only differential path is important) and outputs this correction to the appropriate OPD correction devices.

The fringe data from the OPD control loop in either hardware phase tracking mode or hardware coherencing mode will be archived in order to allow for “software phase tracking”, in which offline “phase rotation” of the science instrument fringe data using contemporaneous FT information can allow for software integration of the science fringe data.

The control loop sampling rate is variable depending on the fringe-tracking mode and the seeing. For cophasing, the sampling time will vary between 0.7 ms and 10 ms, while for the coherencing the sampling time will vary between 5 ms and 50 ms.

The bulk of the analysis of the pixel data can be factored into a simple matrix multiply. For the 6-telescope system the worst-case computation will consist of approximately 1000 multiply-and-accumulate operations. This can be accomplished on a single-processor 1-GHz Pentium in approximately 1 microsecond — far less than the required total latency where the goal is of order $100\mu s$. A standard ESO CPU board should therefore be able to provide the necessary computing power providing that the I/O latency from the detector and system software overheads can be reduced to acceptable values.

8.6 OPD correction

The OPD correction for each telescope is envisaged as being split between a high-frequency correction by an OPD compensator internal to VSI and a low-frequency offload to the VLTI delay lines. The internal compensator will be a piezo-mounted mirror with a bandwidth of at least 700Hz. The stroke of the compensator will depend on the latency of the link to the VLTI delay lines, but is likely to be approximately 10 microns. As a conservative approach, we fix for the OPD compensator the specifications below:

linear range: $100\mu m$

linear resolution: $0.01\mu m$


update rate: $< 1KHz$

9 System performance

The potential performance of the FT are analysed taking into account instrumental factors and the current performance of VLTI. The instrumental contribution, (i.e. system optical throughput, visibility loss, thermal background and detector noise) is evaluated considering the FT set-up described above; the contribution from components deployed along the VSI common path are also included in the overall instrument throughput.

The instrument’s elements considered are the following:

- Beam distribution through VSI switchyard (RD5, Figure 1)

	Fringe Tracker Design for VLTI Spectro-Imager	Rep: 87/2007 Issue: 1.0 Date: 9-11-2007
---	--	---

- ADC and wavelength selection in VSI common path (Figure 3)
- Planar minimum redundancy combiner (Sect.6.2)
- Temporal modulation
- Fibre feeding optics (Sect.6.3)
- HAWAII-1 detector
- H or K band spectrally dispersed across 3 pixels (Sect. 6.5)

9.1 Optical throughput budget

The optical components are assumed to exhibit the following figures:

1. 2% loss at every reflection
2. 2% loss at every AR-coated air/glass surface
3. 1% internal loss in every transmissive component
4. 48%/52% transmission/reflection (worst-case) at every beamsplitter-coated surface
5. The spectrograph optical tolerances are such that a line of detector pixels catches 95% of the flux from a broadband point source
6. 60% detector QE

The elements relevant to the system throughput are summarised below, they account for the surfaces and transmissive media every beam encounters from the VSI common path assembly up to the detector.

Common path elements

- **OPD compensator:** 4 reflecting surfaces at 45 degree incidence
- **Switchyard:** 1 reflecting surface at 45 degree incidence
- **Wavelength selection:**
 - J/H arm: 2 reflections (dichroic + folding mirror) at 45 degree incidence; 1 transmissive component (ADC) equivalent to 4 air-glass interfaces and 4 cm glass thickness.
 - K arm: 1 transmissive optics (dichroic) equivalent to 2cm glass thickness and 2 air-glass interfaces; 2 reflections (folding mirrors) at 45 degree incidence.



Fringe Tracker Design for VLTI Spectro-Imager

Rep: 87/2007
Issue: 1.0
Date: 9-11-2007

FT elements

- Beam Combiner:

- 1 transmissive element (beam splitter / beam combiner): 4cm glass,
- 1 reflection (folding mirror)
- 4 Air-Glass interfaces (2 beamsplitters , 2 beamcombiners)

- **Fibre Optics:** 1 reflection (off axis parabola) and 2 fibre ends

- Dewar Optics:

- 3 transmissive elements in spectrograph (2 doublets and prism) equivalent to 6cm glass
- 6 Air/Glass interfaces in spectrograph

The total elements affecting the system throughput in the spectral band of interest are summarised in the table; relevant to the WFE budget (see below), 7 out of 10 reflections occur at 45 degree of incidence.

Wavelength	H	K
N. Reflections	10	10
N. Air/Glass Interface	14	11
Glass thickness[cm]	12	10
Total internal losses	0.55	0.59

Table 1: FT surfaces and transmissions

Relevant to spatial wavefront quality in the spatial filtering regime - FT working condition - in which the beams are spatially filtered after beam combination, the coupling of the beams into the spatial filter is reduced but the rms fringe contrast is restored to approximately unity. For beams with rms wavefront aberrations of σ , the transmission is reduced by approximately $\exp(-\sigma^2)$; $\lambda/10$ optic figure (peak-to-valley wavefront error at 633nm laboratory source) is equivalent to $\lambda/50$ rms error, i.e. 13nm. In the configuration of the FT, there are from 13 to 10 optics, respectively for the H band K band, before the spatial filter, and reflection would occur at 45 degree of incidence upon 7 out of 10 surfaces. The resulting rms wavefront quality is 106nm in H and 104nm in K, corresponding to a 0.83 loss in spatial-filter throughput at $1.6 \mu\text{m}$ and 0.91 at $2.2 \mu\text{m}$. All the above figures refer to high-order wavefront errors, i.e. neglecting tip/tilt. Tip/tilt errors are dependent on system alignment and drift and are harder to quantify, as they depend on the details of system implementation. As a placeholder, we adopt a 5% error budget value for the throughput loss due to tilt misalignments, and a further 2% loss due to pupil misalignments.

The total system throughput and contributions are recapitulated in Table 2.

9.2 System visibility

Several effects contribute to a loss of fringe contrast.



Fringe Tracker Design for VLTI Spectro-Imager

Rep: 87/2007
Issue: 1.0
Date: 9-11-2007

Wavelength	H	K
Surface and transmission losses	0,55	0,59
Spatial filtering coupling loss for 100% Strehl wavefront	0,80	0,80
Spatial filtering coupling loss due to high-order WFE	0,83	0,91
Reflection losses, fibre ends	0,9	0,9
Coupling loss to spatial filter: tip/tilt misalignments	0,95	0,95
Coupling loss to spatial filter: pupil misalignments	0,98	0,98
System transmission	0,31	0,37
Spectrograph-pixel coupling	0,95	0,95
Detector QE	0,60	0,60
FT total throughput	0,18	0,21

Table 2: FT optical throughput

Spatial wavefront errors and pupil misalignments have already been taken care of by assuming near-perfect spatial filtering; so, the visibility losses associated with these have been converted into intensity losses.

Piston jitter is hard to quantify and it is implementation-dependent. It is likely to be small.

Beam intensity mismatches are likely to arise from mismatches in the transmission and reflection coefficients of the beamsplitter and beamcombiner. The worst case transmission/reflection unbalance accounts for a negligible degradation in visibility, less than 1% .

Polarisation effects , i.e. state mismatch polarisation-dependent phase shift, are likely to arise from mismatches in glass thicknesses, errors in beam-splitter/beam-combiner and AR-coating performance. Polarisation state unbalance arising at BS/BC interfaces does not affect significantly fringe contrast; 2% conservative intensity mismatch corresponds to a visibility loss largely less than 1%. The phase shift between superposing polarisation components is considered the most significant degradation factor; fringe contrast at level of 97% is compatible with conservative, worst case phase difference between superposing polarisation components of 30 degree. The combined effects of these terms have been measured in a prototype combiner built in Cambridge, and in broadband unpolarised light, the losses were measured at less than 5%. This is largely thanks to the low angles of incidence on the coatings.

From the above considerations, the FT visibility can be conservatively estimated at the value of 95%.

9.3 Read noise

The adopted RON figure is the one quoted for the HAWAII detector operated in CDS readout mode, i.e 15 electrons rms per read.

	Fringe Tracker Design for VLTI Spectro-Imager	Rep: 87/2007 Issue: 1.0 Date: 9-11-2007
---	--	---

9.4 Thermal background

The combination of the telescope, sky background and all the warm optics in the beam train are modelled as a single blackbody at approximately 300K. A 300K blackbody source emits $3.64 \star 10^{15}$ photons/second/sr/m² over the K bandpass (2.04-2.37 μ m). In the spatial filtering regime by a fibre diameter D which is exactly matched to the first Airy ring of the diffraction limited spot corresponding to that pupil, the beam etendue is given by

$$\pi(1.22\lambda/D)^2\pi(D/2)^2 \simeq 3.67\lambda^2 \quad (1)$$

In K band, effective wavelength 2.2 μ m, this translates to $6.9 \star 10^4$ photons/s in the system per beam. In spite of the stellar beam splitting, the background flux is not divided by two, because background from the laboratory adds to the stellar beam at the beamsplitter.

9.5 SNR calculation

The measurement SNR potentially achievable by the FT is evaluated within the computational framework described in VSI memo VSI-SYS-001 and through the formula below:

$$SNR = \frac{N_{AC}^2 V^2}{\sqrt{\sigma_{ph}^2 + \sigma_{det}^2}}, \quad (2)$$

N_{AC} is the number of coherent source photons effectively employed in the fringe measurements, i.e. the modulated part of the fringe signal. In a pair-wise combination, it is formed by the correlation of the fraction α of the beams coming from the two given apertures; assuming all apertures receive the same amounts of photons N, $N_{AC} = 2\alpha N$.

V is system visibility, inclusive visibility loss from VLTI infrastructure.

N_{DC} is the number of incoherent photons due to the source, i.e. the signal continuum which is subtracted but contribute to the noise. It is the sum of all beams coming from contributing telescopes n_T , i.e. $N_{DC} = n_T \alpha N$, with n_{DC} the number of telescopes contributing to the DC part: in a pair-wise combination $n_T = 2$.

The noise terms σ_{ph} and σ_{det} are respectively the photon noise from the source and the background, and the total read-out noise:

$$\sigma_{ph}^2 = (N_{DC} + N_{BG})^2 + 2(N_{DC} + N_{BG})N_{AC}^2 V^2; \quad \sigma_{det}^2 = 2n_p^2 \sigma_e^4. \quad (3)$$

N_{BG} is the number of background photons, σ_e is the read-out noise per pixel and n_p is the number of pixel to be involved in the measurement.

With respect to the SNR expression and computational framework it refers to, the involved quantities must be computed taking into account the instrumental parameters (see above) and the details of implementation of the beam combination.

In pair-wise nearest-neighbour combination scheme, each beam is split in two equal intensity fractions, then each measurement channel receives half the photons N collected by single aperture. Therefore, for the sake of the SNR computation, $n_T = 2$, independently from the total number of telescopes combined, and $\alpha = 1/2$; then, $N_{AC} = N$ and $N_{DC} = N$ as well.



Fringe Tracker Design for VLTI Spectro-Imager

Rep: 87/2007
Issue: 1.0
Date: 9-11-2007

The total number of pixels depends upon the details of fringe tracking algorithm implementation: for the ABCD coding with 3 spectral channels, the usage of the whole spectral band imposes to read three times the number of pixels involved into signal phase coding; so, the effective number of pixels to read is 12.

Photon flux at the entrance of the fringe tracker is computed starting from top atmosphere zero magnitude flux collected by the UT pupil, and assuming the VLTI performance reported in VLTI ICD document (AD2) The VLTI relevant figures used in the evaluation are summarised in Table 3.

Wavelength	H	K
Zero-mag top atmosphere flux(UT case)[ph/s]	1.52 10(11)	8.4 10(10)
Atmospheric transmission	0.97	0.90
VLTI Strehl Ratio (MACAO, V=13)	0.39	0.47
Strehl Ratio loss(21 mas tip/tilt residual)	0.68	0.81
VLTI Throughput	0.11	0.12
VLTI Visibility(0.5 ms piston jitter)	0.9	0.95
VLTI Visibility(5 ms piston jitter)	0.8	0.9
VLTI Visibility(10 ms piston jitter)	0.7	0.8

Table 3: FT optical throughput

The resulting performance with UTs are presented in Figure 8, where the achievable SNR in H and K band is shown as a function of the magnitude. The Table 4 summarises the expected FT limiting figures in working bands and in operating regimes likely to be applicable to cophasing or coherencing.

T_{exp} [ms]	H		K	
	SNR=5	SNR=3	SNR=5	SNR=3
0.5	6.9	7.9	8.0	8.5
1.0	7.6	8.5	8.7	9.2
5.0	9.3	10.2	10.4	10.9
10.0	9.8	10.8	10.9	11.5

Table 4: FT Limiting magnitude in H and K

Fringe tracking at fainter magnitudes is potentially achievable through the incoherent coherencing, where the group delay is integrated incoherently over many coherent integrations performed in starved photon regime. It is demonstrated that the group delay tracking is possible down to SNR values per integration of approximately 0.7 (Buscher PhD Thesis, University of Cambridge, 1988). A conservative performance estimate in photon starved regime can be obtained by the framework and provisions above: assuming 20 ms incoherent integration and a SNR=1, associated to the single coherent integration, the FT limiting magnitudes are roughly close to H=12.7 and K=13.2.

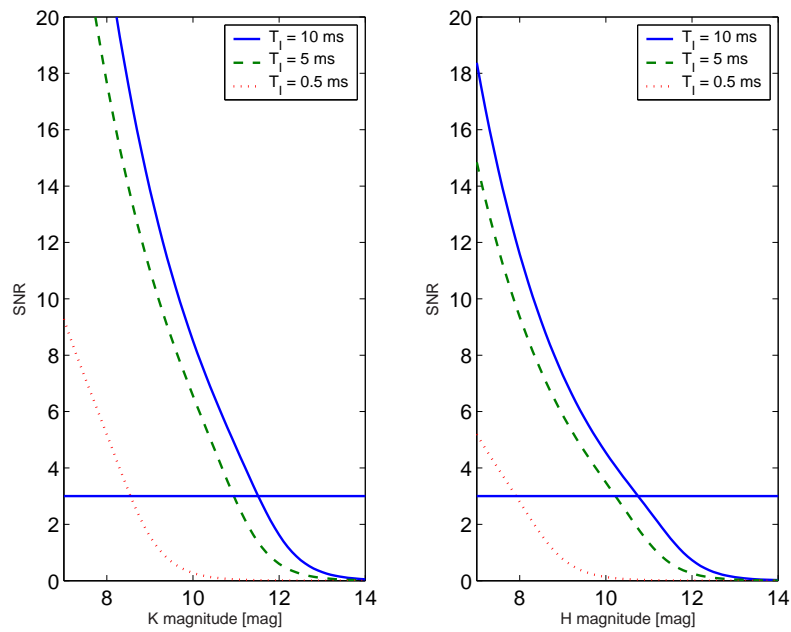


Figure 8: Fringe Tracker SNR performance as a function of magnitude: horizontal line corresponds to $SNR = 3$